




Article

Electro-Fenton-Based Technologies for Selectively Degrading Antibiotics in Aqueous Media

Ángela Moratalla ¹, Engracia Lacasa ², Pablo Cañizares ¹, Manuel A. Rodrigo ¹ and Cristina Sáez ^{1,*}

¹ Department of Chemical Engineering, Faculty of Chemical Sciences and Technologies, University of Castilla-La Mancha, 13005 Ciudad Real, Spain; angela.moratalla@uclm.es (Á.M.); pablo.canizares@uclm.es (P.C.); manuel.rodrigo@uclm.es (M.A.R.)

² Department of Chemical Engineering, Higher Technical School of Industrial Engineering, University of Castilla-La Mancha, 02071 Albacete, Spain; engracia.lacasa@uclm.es

* Correspondence: cristina.saez@uclm.es

Abstract: The viability of the Electro-Fenton (EF) process in the selective degradation of penicillin G (PenG) in complex solutions has been studied. The role of the anode material (boron-doped diamond (BDD) or mixed metal oxide (MMO)) and the cathode 3D support (foam or mesh), as well as the synergistic effect of UVC light irradiation (photoelectron-Fenton, PEF), have been evaluated. The results show that Pen G can be efficiently and selectively removed by EF, obtaining higher PenG removal rates when using the BDD anode (100%) than when using the MMO anode (75.5%). Additionally, mineralization is not favored under the experimental conditions tested (pH 3, 5 mA cm⁻²), since both aromatic and carboxylic acids accumulate in the reaction system as final products. In this regard, the EF-treated solution presents a high biological oxygen demand and a low percentage of *Vibrio fischeri* inhibition, which leads to high biodegradability and low toxicity of this final effluent. Furthermore, the combination with UVC radiation in the PEF process shows a clear synergistic effect on the degradation of penicillin G: 166.67% and 83.18% using MMO and BDD anodes, respectively. The specific energy required to attain the complete removal of PenG and high inhibition of the antibiotic effect is less than 0.05 Ah dm⁻³. This confirms that PEF can be efficiently used as a pretreatment of conventional wastewater treatment plants to decrease the chemical risk of complex solutions polluted with antibiotics.

Keywords: mixed metal oxide; diamond electrode; hydrogen peroxide; toxicity; biodegradability; antibiotic; Electro-Fenton



Citation: Moratalla, Á.; Lacasa, E.; Cañizares, P.; Rodrigo, M.A.; Sáez, C. Electro-Fenton-Based Technologies for Selectively Degrading Antibiotics in Aqueous Media. *Catalysts* **2022**, *12*, 602. <https://doi.org/10.3390/catal12060602>

Academic Editors: Aida M. Díez and Vitor J. P. Vilar

Received: 5 May 2022

Accepted: 30 May 2022

Published: 31 May 2022

Publisher's Note: MDPI stays neutral with regard to jurisdictional claims in published maps and institutional affiliations.



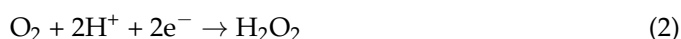
Copyright: © 2022 by the authors. Licensee MDPI, Basel, Switzerland. This article is an open access article distributed under the terms and conditions of the Creative Commons Attribution (CC BY) license (<https://creativecommons.org/licenses/by/4.0/>).

1. Introduction

Pharmaceutical compounds (PhCs) are considered potentially hazardous substances due to their chemical and bioactive behavior in aquatic environments [1]. Depending on their characteristics and therapeutic actions, PhCs can be divided into different categories, such as antiepileptic, anti-inflammatory, antipyretic, antibiotic, β -blocker and psychiatric drugs [2]. Antibiotics are the most frequently detected in the environment, and benzylpenicillin, or penicillin G (PenG), is a persistent chemical compound in the aquatic environment that shows nonbiodegradable behavior and a high level of toxicity to *Vibrio fischeri* and *Daphnia Magna* [3,4]. The antimicrobial nature of antibiotics precludes their effective removal in conventional wastewater treatment plants (WWTPs) [5,6]. Furthermore, the range of detected concentrations may be larger depending on the type of effluent. In hospitals, the concentration of antibiotics is approximately 25% higher than that in municipal wastewater [7].

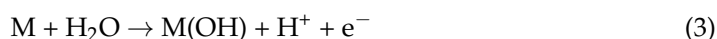
Over the last few years, advanced oxidation processes (AOPs) have demonstrated high performance and efficiency in the removal of PhCs in wastewater, such as ozonation, ultraviolet irradiation, TiO₂ photocatalysis and the Fenton process [8–11]. These technologies

promote the generation of oxidizing agents with high reactivity. Among AOPs, electrochemical advanced oxidation processes (EAOPs) allow the generation of these species from in situ oxidation and reduction reactions without the addition of chemicals for the removal of organic substances [12–15]. Thus, the Electro-Fenton (EF) process, as a type of EAOP, is currently a major area of interest due to its excellent efficiency and ease of operation. It is based on the production of hydroxyl radicals through the Fenton reaction (Equation (1)) at pH 3 between the electrogenerated hydrogen peroxide (H_2O_2) by the reduction of oxygen (Equation (2)) at the cathode and the iron catalyst.



The efficiency of the EF process depends on the availability of both H_2O_2 and Fe^{2+} . The formation of iron sludge due to the use of homogeneous catalysts, which is difficult to treat and can lead to secondary pollution [16], is an important drawback of this process. To solve this problem, some authors have employed heterogeneous catalysts to implement the heterogeneous EF process [17] using fluidized beds [18–20]. Regarding the generation of hydrogen peroxide during the electrochemical process, two factors are critical: the proper selection of the cathodic material and the availability of oxygen to be reduced. Carbonaceous materials such as graphite, carbon felt or carbon cloth have demonstrated very good performance for the efficient production of hydrogen peroxide [21,22], mainly when they are modified with a mixture of carbon black (CB) and polytetrafluoroethylene (PTFE) [23]. However, the implementation of carbonaceous materials in the scale up of flow-by reactors or microfluidic flow-through reactors (MF-FT) is still an important drawback. At this point, the use of 3D metallic materials that can be easily modified with a CB/PTFE mixture may be an attractive alternative to the cathode materials commonly used at the lab scale [24]. In addition, another critical limitation that makes EF difficult to apply on a large scale is the limited solubility of oxygen in water at atmospheric pressure [14,23,24]. An interesting alternative evaluated in previous works is the use of a jet aerator based on the Venturi effect to ensure supersaturation in oxygen of the electrolyte [21,25].

The overall performance of EF can be significantly improved by combination with AOPs. Then, the proper selection of the anodic material that promotes hard soft oxidation conditions, depending on the treatment goal, is also a very relevant parameter to take into consideration. At this point, it is important to note that nonactive anodes (such as conductive diamond electrodes) promote the generation of quasi-free hydroxyl radicals (Equation (3)) near the electrode surface [26–28], and those radicals can overlap the cathodic area and oxidize $\text{H}_2\text{O}_2/\text{Fe}^{2+}$. Additionally, it is well-reported that, depending on the anode material and the experimental conditions selected (mainly current density), the formation of other reactive species from the oxidation of salts contained in the target solutions can occur, and if they are properly activated, they can also contribute to the overall degradation process. In the search for synergies between processes, some authors have studied the effect of the coupling of light on the EF process. Thus, the photoelectron-Fenton process (PEF) can transform H_2O_2 into hydroxyl radicals due to the photolysis of molecules (Equation (4)) using UVA ($\lambda_{\text{max}} = 365 \text{ nm}$), solar irradiation or UVC ($\lambda_{\text{max}} = 254 \text{ nm}$) [29,30]. In addition, UV light can be degraded by the direct photolysis of aromatic molecules [31].



Within this framework, this paper is focused on the evaluation of heterogeneous EF-based technologies to decrease the chemical risk from hospital urines as a pretreatment before their disposal into municipal sewers. The influence of the anode material (boron-doped diamond (BDD) or mixed metal oxide (MMO)), the cathode support (foam or mesh) and the synergistic effects of irradiating UVC light on the EF process have been

studied to degrade PenG as a model of target antibiotics. However, the main novelty of this work is not the complete mineralization of the effluent, but the selective degradation of the antibiotic into other compounds with lower antibiotic activity and toxicity to increase the biodegradability of the treated effluent. To perform this, the toxicity (using a marine bacterium, *Vibrio fischeri*), antibiotic activity (using *Enterococcus faecalis*) and biodegradability (using real sewage sludge) were evaluated during electrochemical treatment.

2. Results and Discussion

Figure 1 shows the evolution of the PenG concentration with the applied electric charge during the EF tests (working at 5 mA cm^{-3} and using 10.8 g of goethite as a heterogeneous catalyst) in synthetic urine media. For comparison purposes, sodium sulfate was also tested as a typical supporting electrolyte due to the complexity of the urine medium (a mixture of organic and inorganic salts as well as simple organic compounds). Additionally, the toxicity (with regard to the inhibition percentage of bioluminescence from *Vibrio fischeri*) and the biological oxygen demand ($\text{BOD}_{5\text{T}}$) of the solutions are shown.

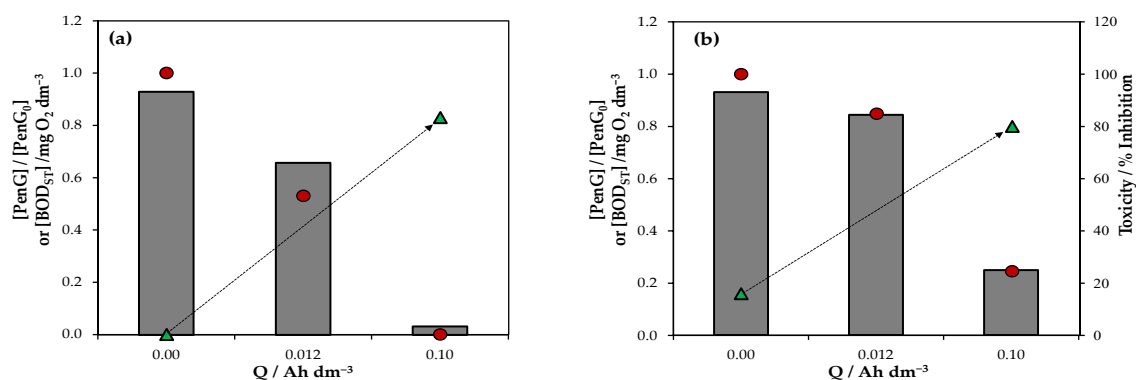


Figure 1. Changes in the concentrations of PenG (●), $\text{BOD}_{5\text{T}}$ (▲) and toxicity (grey bars) during the EF treatment of (a) sulfate or (b) synthetic urine solutions polluted with PenG. Initial PenG concentration: 50 mg dm^{-3} , pH_0 : 3.0, anode: $\text{MMO-IrO}_2\text{Ta}_2\text{O}_5$, cathode: titanium foam with CB/PTFE, 10.8 g of goethite. Current density: 5 mA cm^{-3} .

PenG can be efficiently removed by EF, but the efficiency and degradation rate depend on the supporting electrolyte media. After passing 0.10 Ah dm^{-3} of electric charge, the complete degradation of PenG is attained in a pure sulfate medium, while approximately 25% of PenG still remains in the urine medium. The lower efficiency in this complex aqueous solution is related to the competitive degradation of PenG with other organics present in the solution, such as uric acid, urea and creatinine. The evolution of those organics with the applied electric charge is shown in Figure S1. Herein, Table 1 shows the kinetic degradation constants (k, min^{-1}) of PenG and other organics in both reaction media tested. These values are obtained by fitting the data to a first-order kinetic model according to Equation (5), where t is the time and C_0 and C are the concentrations (in mg dm^{-3}) at the initial or a given time, respectively. The degradation of PenG is three times faster in the sulfate medium than in urine (0.0092 min^{-1} vs. 0.0028 min^{-1}). Otherwise, uric acid is the most rapidly degraded organic compound in urine, with a kinetic constant approximately two times higher than that of PenG (0.0064 min^{-1} vs. 0.0028 min^{-1}) [32]. These results agree with those found in the literature. Feng et al. [15] observed that the removal of 0.08 mM piroxicam was faster in tap water than in hospital wastewater (HWW) or urine media during the EF process (using BDD and 3D carbon felt as the anode and cathode, respectively).

$$\ln(C/C_0) = -k \cdot t \quad (5)$$

Table 1. Kinetic constant of degradation of organics during EF of PenG solutions in sulfate or urine.

Compound	Electrolyte	k/min ⁻¹
PenG	Na ₂ SO ₄	0.0092
PenG	Urine	0.0028
Uric Acid	Urine	0.0064
Creatinine	Urine	0.0005
Urea	Urine	0.0002

Regarding biological parameters, it can be observed that the toxicity decreases during the EF process. The possible interferences related to the electrogenerated oxidants (such as hydrogen peroxide, hypochlorite or chlorate) were neutralized with sodium thiosulfate (with a ratio of mol oxidants quantified by I⁻ /I₂ titration to 1 mol sodium thiosulfate). Then, the toxicity only informs about the sensitivity of *Vibrio fischeri* to the organics (PenG and other metabolites) present in the solution. According to the obtained results, in the sulfate medium, the final percentage of inhibition is almost zero, while it remains at approximately 25% in the urine medium, which seems to be directly related to the remaining PenG concentration.

To shed light on the chemical risk of EF-treated urine, the biological oxygen demand (BOD_{ST}) of the polluted solutions was also determined using a short biodegradability test described elsewhere [33]. It consists of monitoring the changes in the oxygen consumption of microorganisms contained in an activated sludge (collected from the wastewater treatment plant of Ciudad Real) when the samples of the target solutions (initial or EF-treated in both reaction media) are added. The results obtained in this short biodegradability test are illustrated in Figure 2. The profile of the oxygen concentration observed during approximately the first 900 s corresponds to the endogenous respiration of the sludge. After that, the target solution is added, and the decay varies from linear to exponential, which is related to the substrate contained in the sample. Once this substrate is consumed, the oxygen consumption rate returns to endogenous respiration, and the decay slope returns to its initial value. Then, the difference between the dissolved oxygen values of the endogenous sludge phase before and after the addition of the sample informs about the mg dm⁻³ of the oxygen consumed for substrate degradation. Thus, as more oxygen is consumed, the substrate becomes more biodegradable.

The initial urine shows slight biodegradability (0.16 mg O₂ dm⁻³) related to the contained urea and other simple organics, but it is zero in the case of the sulfate solution, where PenG is the sole organic contained in the solution. In both cases, after EF treatment, there is a clear increase in the BOD_{ST} until 0.80 and 0.83 mg O₂ dm⁻³ in urine and sulfate media, respectively. These results confirm that EF treatment degrades PenG into less recalcitrant and more biodegradable compounds. In fact, EF improves the short-term biological oxygen demand of the target solutions.

As stated before, the generation of hydrogen peroxide from the reduction of oxygen (Equation (2)) during the electrochemical process may limit its efficiency, since the proper selection of the cathodic material is a critical factor. In this work, two Ti-supporting materials (3D titanium foam and 3D titanium mesh) with different geometries and porosities but with the same deposition of carbon black/PTFE [34] are tested. Figure 3 shows the percentage removal of PenG and the increment in the BOD_{ST} attained by EF using both cathodic supports. Additionally, the performance of two types of anodes (MMO and BDD) is tested to evaluate the contribution of the anodic reactions in the direct and/or mediated degradation of PenG in complex aqueous solutions.

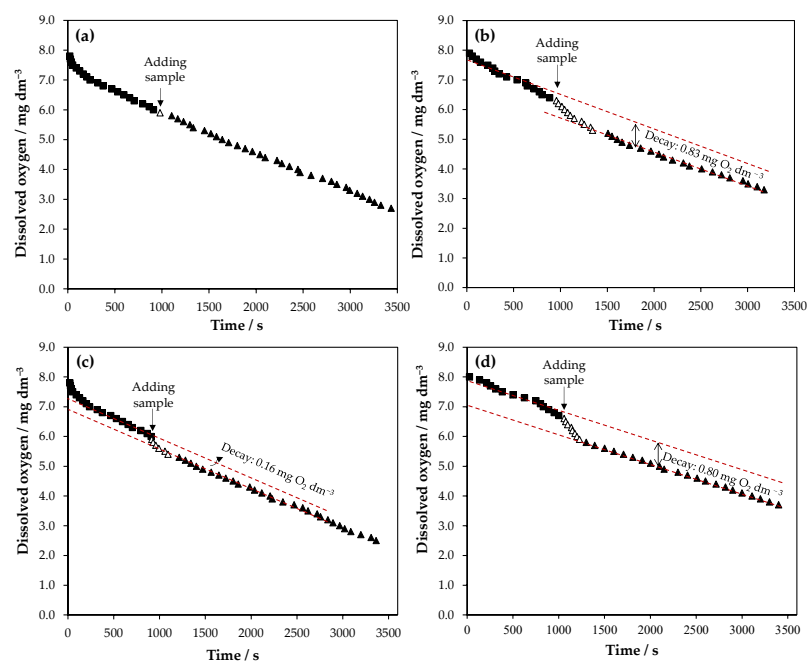


Figure 2. Dissolved oxygen as a function of time for the initial and final samples of the EF tests: (a) initial sample in sulfate; (b) final sample in sulfate; (c) initial sample in urine; (d) final sample in urine. Current density: 5.0 mA cm^{-3} , pH_0 : 3.0, anode: MMO, cathode: titanium foam with CB/PTFE, 10.8 g of goethite. Legend: (■) endogenous phase before the addition sample, (Δ) exponential decay associated with substrate degradation, (\blacktriangle) endogenous phase after the addition sample.

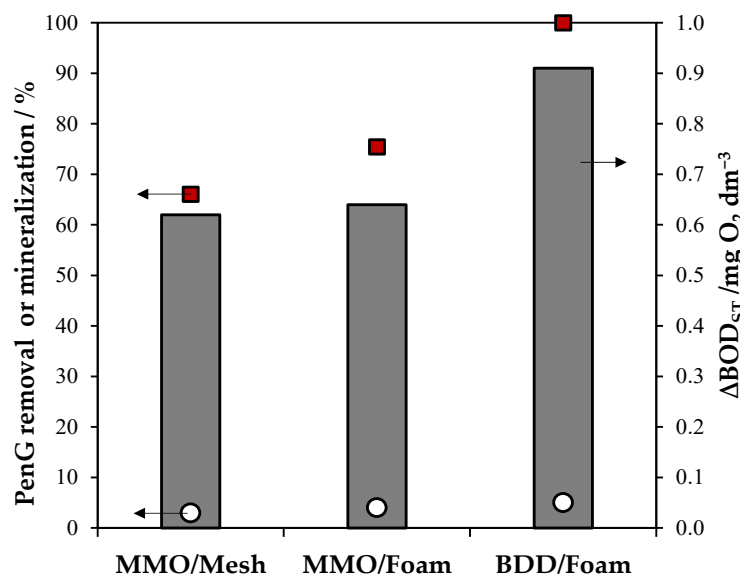


Figure 3. Pen G removal (■), mineralization (○) and $\Delta\text{BOD}_{\text{ST}}$ (grey bars, ■) of urine treated by EF using different combinations of electrode materials (anode/cathode): MMO/Ti mesh, MMO/Ti foam, BDD/Ti foam. Initial PenG concentration: 50 mg dm^{-3} , current density: 5 mA cm^{-3} , pH_0 : 3.0, 10.8 g of goethite. Electric charge passed: 0.1 Ah dm^{-3} .

As can be observed, the influence of the Ti support used as the cathode is less relevant than the type of anode tested. In fact, PenG removal is slightly higher when titanium foam is used as the cathodic support (75.5% vs. 66.1%) with the MMO anode. This better performance may be related to the higher contact surface of Ti foam and the slightly higher electrogeneration of hydrogen peroxide: $9.1 \text{ vs. } 9.6 \text{ mg dm}^{-3}$ (values attained operating the system at the same current density but in absence of an iron catalyst).

Regarding the effect of the anodic material, the complete removal of PenG is attained using BDD, but mineralization remains at very low percentages (below 5%). This is an unexpected result, since the typical high mineralization reported with BDD electrolysis is generally carried out at current densities above 30 mA cm^{-2} [11,34,35]. Cotillas et al. [35] reported that it was possible to attain complete removal of 100 mg dm^{-3} in urine when working with BDD or MMO anodes (at current densities of 10 and 100 mA cm^{-2}) by the EO process, where the BDD anode was more efficient than MMO. Furthermore, Herraiz-Carboné et al. [36] compared the use of BDD and MMO, not only for the degradation of 100 mg dm^{-3} chloramphenicol (antibiotic), but they also looked at the toxicity and biodegradability behavior of the urine treated with the EO process. They reported that the EO process with BDD decreases the hazardousness of hospital urine at low current densities (1.25 mA cm^{-2}) and an electric charge of 8 Ah dm^{-3} . This means that, under the soft oxidation conditions used (5 mA cm^{-3} and pH 3), the partial degradation of the antibiotic is favored, and the mineralization of the other organics present initially in the urine is not promoted. Another important observation is that this PenG removal corresponds to an increment of 90% in the biodegradability of the target urine (65% in the case of using the MMO anode). All these results indicate that, although neither organic compounds naturally contained in the urine nor PenG are completely degraded to carbon dioxide, the intermediates accumulated in the system are much less recalcitrant than PenG. Thus, EF can be used as a pretreatment for biological processes (typically implemented in WWTPs).

However, one of the main chemical risks associated with aqueous wastes polluted with antibiotics is their antibiotic effect. Evidently, this is associated with the concentration of the target antibiotic, but it may also be related to some of its metabolites or degradation intermediates. To confirm this, the antibiotic effect of the treated urine was measured indirectly by comparing the effect of the addition of the treated and nontreated urine on a culture of *E. faecalis* (selected as reference bacteria due to its high sensitivity to PenG). Likewise, a reference test in the absence of antibiotics is carried out to confirm that *E. faecalis* is not sensitive to other compounds naturally present in the urine. Figure 4 shows the percentage of inhibition of *E. faecalis* as well as that of *Vibrio fischeri*, used as indicators of the antibiotic effect and toxicity of the treated urine, respectively. For comparison purposes, values of the untreated urine polluted with PenG are also included in the figure.

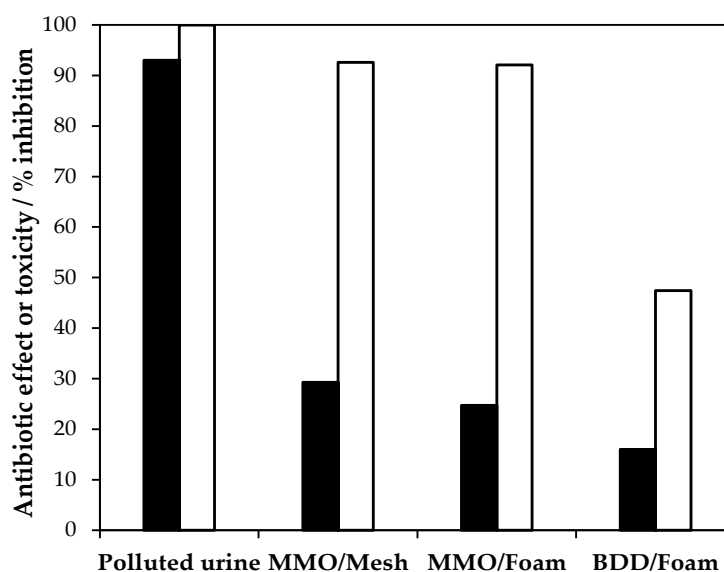


Figure 4. Antibiotic effect (white bars, □) and toxicity (black bars, ■) of the urine treated by EF using different combinations of electrode materials (anode/cathode): MMO/Ti mesh, MMO/Ti foam, BDD/Ti foam. Initial PenG concentration: 50 mg dm^{-3} , current density: 5 mA cm^{-3} , pH₀: 3.0, 10.8 g of goethite. Electric charge passed: 0.1 Ah dm^{-3} .

As expected, the initial polluted urine shows the maximum percentage of inhibition of both target bacteria due to its initial PenG concentration (50 mg dm^{-3}). After EF treatment, the toxicity decreases to 30–115%, depending on the electrodes used. However, *E. faecalis* inhibition remains above 90% when MMO is used as the anode and only decreases below 45% during BDD-EF. These results should only be related to the organic composition of the treated urine since the electrogenerated oxidants are neutralized with thiosulfate. In the case of BDD-EF, the complete depletion of PenG is attained (see Figure 3), but the treated urine maintains a certain antibiotic character, despite its higher biodegradability and lower toxicity. Herein, the intermediates formed during the EF processes are identified by LC–MS. Table 2 shows the most complex intermediates detected during the EF processes with MMO and BDD, and Figures 5 and 6 show their profiles as well as those of carboxylic acids (all of them are expressed with regard to chromatographic area).

Table 2. Analytes identified, structure and m/z.

	Anode	Formula	Feasible Structure	m/z
Pen G	-	$\text{C}_{16}\text{H}_{18}\text{N}_2\text{O}_4\text{S}$		334.0987
M1	MMO/BDD	$\text{C}_{16}\text{H}_{18}\text{N}_2\text{O}_5\text{S}$		353.1171
M2	MMO/BDD	$\text{C}_{16}\text{H}_{20}\text{N}_2\text{O}_5\text{S}$		352.1092
M3	MMO/BDD	$\text{C}_{16}\text{H}_{18}\text{N}_2\text{O}_4\text{S}$		334.0987
M4	BDD	$\text{C}_{15}\text{H}_{18}\text{N}_2\text{O}_3$		274.1317
M5	MMO/BDD	$\text{C}_{10}\text{H}_{15}\text{NO}_2\text{S}$		213.0824
M6	BDD	$\text{C}_{14}\text{H}_{16}\text{N}_2$		212.1314
M7	BDD	$\text{C}_{11}\text{H}_{13}\text{NO}_2$		191.0946

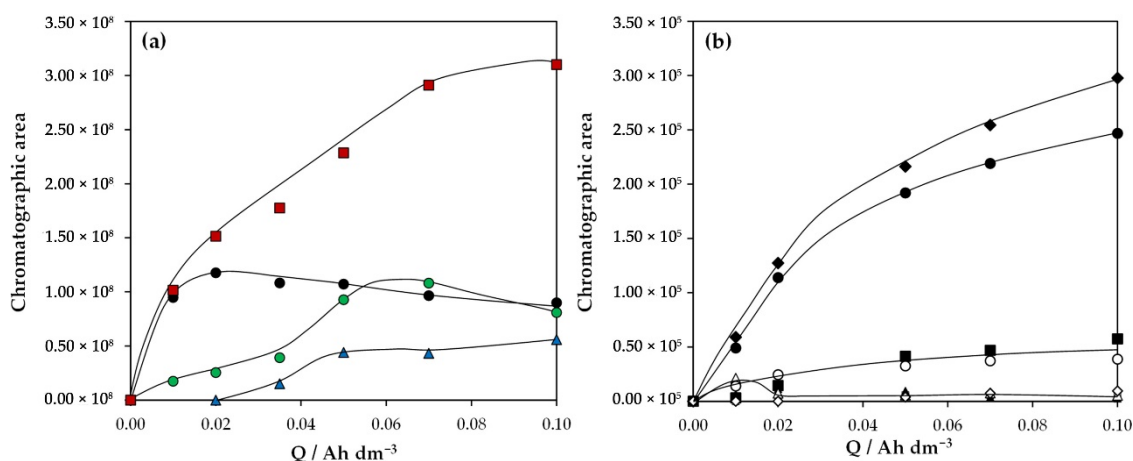


Figure 5. Chromatographic area of different compounds as a function of the applied electric charge during the degradation of PenG in urine by the EF process with MMO as the anode and Ti foam as the cathode: (a) complex PenG intermediates: (▲) $C_{16}H_{18}N_2O_5S$, (●) $C_{16}H_{20}N_2O_5S$, (●) $C_{16}H_{18}N_2O_4S$, (■) $C_{10}H_{15}NO_2S$; (b) carboxylic acids: (□) oxalic acid, (■) maleic acid, (▲) oxamic acid, (Δ) malonic acid, (●) succinic acid, (○) formic acid, (◆) acetic acid, (◇) propionic acid. Initial PenG concentration: 50 mg dm^{-3} , current density: 5 mA cm^{-3} , pH_0 : 3.0, 10.8 g of goethite.

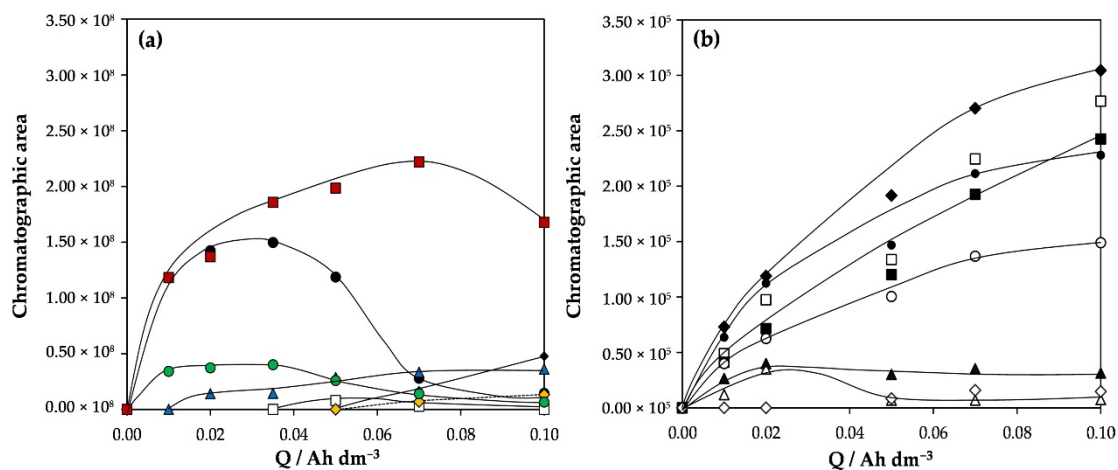


Figure 6. Chromatographic area of different compounds as a function of the applied electric charge during the degradation of PenG in urine by EF process with BDD as anode and Ti-foam as cathode: (a) complex PenG intermediates: (▲) $C_{16}H_{18}N_2O_5S$, (●) $C_{16}H_{20}N_2O_5S$, (●) $C_{16}H_{18}N_2O_4S$, (■) $C_{10}H_{15}NO_2S$, (□) $C_{14}H_{16}N_2$, (◆) $C_{11}H_{13}NO_2$, (◆) $C_{15}H_{18}NO_3$; (b) carboxylic acids: (□) oxalic acid, (■) maleic acid, (▲) oxalic acid, (Δ) malonic acid, (●) succinic acid, (○) formic acid, (◆) acetic acid, (◇) propionic acid. Initial PenG concentration: 50 mg dm^{-3} , current density: 5 mA cm^{-3} , pH_0 : 3.0, 10.8 g of goethite.

As can be observed, the degradation of PenG leads to the accumulation of many compounds with complex structures as well as carboxylic acids. Their concentrations and ratios seem to depend on the nature of the anode. The use of the MMO anode leads to the accumulation of four complex organics ($C_{16}H_{18}N_2O_5S$, $C_{16}H_{20}N_2O_5S$, $C_{16}H_{18}N_2O_4S$ and $C_{10}H_{15}NO_2S$), and three additional organics ($C_{14}H_{16}N_2$, $C_{11}H_{13}NO_2$ and $C_{15}H_{18}NO_3$) are also detected with the BDD anode. In this last case, only one of them shows the typical intermediate profile (formation and accumulation followed by a later degradation). Additionally, in both cases, eight carboxylic acids are detected (oxalic, maleic, oxamic, malonic, succinic, formic, acetic and propionic acids) in the reaction system, and their concentrations are higher when using BDD. Except for malonic acid, all of them remain as the final products of the EF process under the experimental conditions used, which is in

line with the lack of mineralization observed. These results corroborate that, after passing 0.10 Ah dm^{-3} , the partial degradation of PenG is attained, and the degradation progress is greater with BDD, which justifies the higher biodegradability and the lower toxicity and antibiotic effect of BDD-treated urine.

The better performance of the EF system equipped with BDD confirms the important contribution of anodic reactions to the overall electrochemical process, even under the soft oxidation conditions used. At this point, it is important to remark that the EF tests are conducted at a current density of 5 mA cm^{-2} . This value is selected to promote the two-electron oxygen reduction reaction to form H_2O_2 (Equation (2)) and to avoid the four-electron oxygen reduction reaction that leads to the formation of H_2O (Equation (6)) [37,38], and it is far from the typical current density applied in electrochemical oxidation processes ($30\text{--}100 \text{ mA cm}^{-2}$), in which very strong oxidation conditions occur [39]. Under these typical conditions, BDD electrolysis leads to the massive formation of hydroxyl radicals from water oxidation as well as to the generation of a cocktail of oxidants from the direct or hydroxyl radical-mediated oxidation of salts (chloride, sulfate, phosphate or carbonates) contained in the aqueous solution. Using MMO anodes, chlorides are electrochemically oxidized to form hypochlorite, but the formation of highly oxidized chlor species (such as chlorate or perchlorate) or oxidants from sulfate or phosphate ions is not expected. In this case, chlorate and perchlorate are also not detected using BDD. The soft oxidation conditions used did not promote their formation, and hypochlorite and hydrogen peroxide are the main oxidants detected in the reaction system at relevant concentrations.



To evaluate the contribution of the anodic oxidation reaction and oxidants formed, single electrolyses are carried out with MMO and BDD as anodes, and the results are compared with those of the EF process. The PenG removals attained are shown in Figure 7. As can be observed, MMO electrolysis at 5 mA cm^{-2} is not able to degrade PenG, whereas approximately 45% degradation is attained with BDD electrolysis after applying 0.10 Ah dm^{-3} . However, this removal is significantly lower than that attained with EF, indicating the important contribution of the Fenton reagent. In the literature, if the oxidants electro-generated are not activated (chemically or by irradiation), they can remain stable in the solution without contributing to the overall degradation process [40]. Figure 7 also shows the evolution of the PenG concentration during PEF, and for comparison purposes, the results attained by single photolysis are also plotted. To perform this, a UV lamp (9 W, 254 nm) is inserted into the reservoir tank.

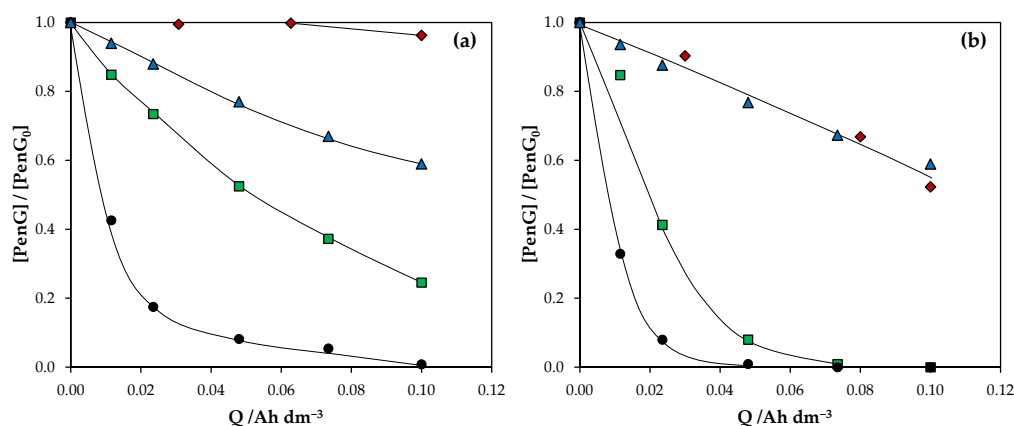


Figure 7. PenG decay as a function of the applied electric charge using MMO (a) and BDD (b) as anodes. (♦) EO, (■) EF, (▲) photolysis, (●) PEF process. Cathode: Ti foam with CB/PTFE, UVC applied in electrochemical processes: 9 W, $j = 5 \text{ mA cm}^{-2}$, $\text{pH}_0 = 3.0$.

The combined PEF process is significantly more efficient than EF and electrolysis, and the specific energy required to attain the complete removal of PenG is less than 0.05 Ah dm^{-3} in the case of using BDD. Regarding the MMO anode, the final percentage of PenG removal increases up to 99.15% during PEF (approximately 75.5% attained in the absence of UV irradiation). Similar results were obtained by Gonzaga et al. [3], who studied the effect of light in the EF process for the removal of PenG (using MMO as the anode and carbon felt as the cathode), although under a higher current density value of 30 mA cm^{-2} . They found that the complete removal of PenG by PEF decreased the toxicity by 96% and completely removed the antibiotic activity. To quantify the effect of the coupling of the different processes, synergy coefficients for PEF were calculated by Equation (7). The kinetic constants of the combined process are summarized in Table 3 as well as the synergy coefficient of PEF and the percentage improvement (in comparison to results attained by EF process) of the microbiological parameter.

$$\text{Synergy coefficient PEF (\%)} = \frac{k_{PEF} - k_{EF} - k_{Photolysis}}{k_{EF} + k_{Photolysis}} \cdot 100 \quad (7)$$

Table 3. Synergy coefficients (%) and percentage of improvement of microbiological parameters of the combined photoelectron-Fenton process in comparison to the Electro-Fenton process.

Process	k/min^{-1}	Synergy Coefficient /%	$\Delta\text{BOD}_{st}/\%$	$\Delta(\text{Toxicity Inhibition})/\%$	$\Delta(\text{Antibiotic Effect Inhibition})/\%$
PEF-MMO/Foam	0.0104	166.67	57.81	23.08	89.00
PEF-BDD/Foam	0.0196	83.18	37.36	18.75	55.00

As can be observed, PEF-MMO/Foam shows a synergy coefficient two times higher than that of PEF-BDD/Foam, which can be related to the better performance of BDD-electrolysis in comparison to MMO electrolysis. On the other hand, the improvement percentages of the microbiological parameters are also higher when MMO is used as the anode in the combined process, obtaining values of 57.81%, 23.08% and 89.00% for DBOD_{st} , toxicity removal and antibiotic effect, respectively. The very relevant improvement attained in regard to the antibiotic effect is in line with the higher removal of both complex intermediates and short chain acids attained by PEF (see Figure 8). Thus, PEF seems to be a very promising technology to decrease the chemical risk of sanitary effluents.

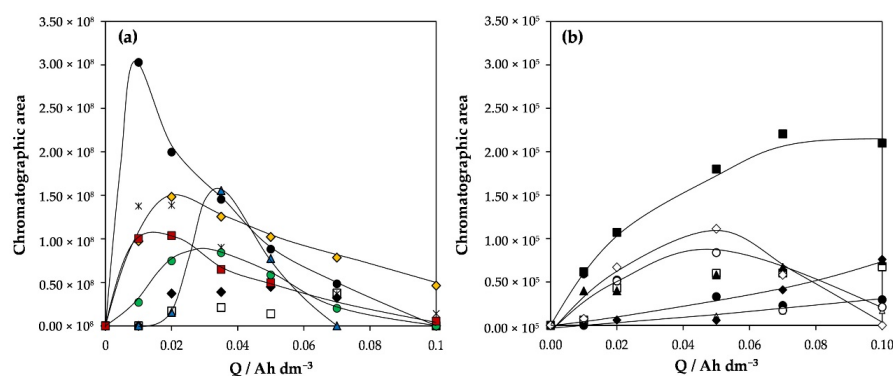


Figure 8. Chromatographic area of different compounds as a function of the applied electric charge during the degradation of PenG in urine by the FEF process with MMO as the anode and Ti foam as the cathode: (a) complex PenG intermediates: (▲) $\text{C}_{16}\text{H}_{18}\text{N}_2\text{O}_5\text{S}$, (●) $\text{C}_{16}\text{H}_{20}\text{N}_2\text{O}_5\text{S}$, (●) $\text{C}_{16}\text{H}_{18}\text{N}_2\text{O}_4\text{S}$, (■) $\text{C}_{10}\text{H}_{15}\text{NO}_2\text{S}$, (□) $\text{C}_{14}\text{H}_{16}\text{N}_2$, (◇) $\text{C}_{10}\text{H}_{11}\text{NO}_2$, (◆) $\text{C}_{15}\text{H}_{16}\text{N}_2\text{O}_2$, (*) $\text{C}_{10}\text{H}_{11}\text{NO}_3$; (b) carboxylic acids: (□) oxalic acid, (■) maleic acid, (▲) oxamic acid, (Δ) malonic acid, (●) succinic acid, (○) formic acid, (◆) acetic acid, (◇) propionic acid. Initial PenG concentration: 50 mg dm^{-3} , current density: 5 mA cm^{-2} , pH_0 : 3.0, 10.8 g of goethite, UVC light 9 W.

3. Materials and Methods

3.1. Chemicals

Penicillin G (penicillin G sodium salt, >98%) is of analytical grade. The reagents needed to make synthetic urine (calcium phosphate, diammonium hydrogen phosphate, sodium carbonate, magnesium sulfate, potassium chloride, uric acid, creatinine and urea) are of analytical grade. HPLC-grade methanol, acetonitrile and formic acid (98%) are used in the mobile phase. P-dimethylaminobenzaldehyde and titanium (IV) oxysulfate (1.9–2.1%) are used as indicators of urea and hydrogen peroxide, respectively. Goethite (catalyst grade, 30–50 mesh) is used as a heterogeneous catalyst in EF tests. All chemicals are supplied by Sigma-Aldrich (Madrid, Spain). Double deionized water (Millipore Milli-Q system, resistivity: 18.2 M Ω cm at 25 °C) is used to prepare all solutions.

3.2. Experimental Setup

Figure 9 shows the experimental setup used in this work that can be easily adapted to be used in EF and PEF processes by introducing a 9 W UVC lamp (254 nm, 225 mm length with 19 mm of external diameter) on the reservoir tank. It is equipped with a jet aerator to provide oxygen to the system and a microfluidic flow-through cell (MF-FT) connected to a fluidized bed with 10.8 g of goethite (used as an iron heterogeneous catalyst). The electrolyte is recirculated at 140 dm^{−3} h^{−1} through the system using a Micropump[®] supplied by Techma GPM s.l.r., Milan, Italy. The fluid velocity throughout the catalyst bed is 0.043 m s^{−1}. Part (b) of this figure shows a detailed scheme of the electrochemical cell. It is a flow-through cell equipped with 3D electrodes. Mixed metal oxide mesh (MMO-IrO₂Ta₂O₅, supplied by Tianode[®], Chennai, India) or boron-doped diamond (BDD) supported on a 3D-niobium mesh (Diachem[®], supplied by Condias GmbH, Itzehoe, Germany) are used as anodes. Moreover, 3D Titanium foam and 3D titanium mesh with a deposition of carbon black (CB, Vulcan XC72 from Carcot Corporation, Alton, UK) and PTFE are used as cathodes (preparation procedure described elsewhere [34]). To decrease the cell voltage, the interelectrode gap (IE) is fixed at 150 μ m. Synthetic urine (2.7 dm^{−3}) consists of a mixture of organic species such as urea, creatinine, uric acid, and inorganic salts such as potassium chloride, magnesium sulfate or diammonium hydrogen phosphate (Table S1). The urine is polluted with 50 mg dm^{−3} of PenG. The initial pH of the solution is adjusted to 3, with no significant changes throughout the experiments.

3.3. Chemical Analysis

PenG and uric acid concentrations are monitored by high-performance liquid chromatography (HPLC) using an Agilent 1200 series (Madrid, Spain) coupled to a DAD detector (Agilent, Madrid, Spain) at 220 nm and 292 nm, respectively. For the determination of PenG concentration, a mixture of 50% methanol and 50% formic acid (0.1%) is used as the mobile phase, with a flow rate of 0.6 mL min^{−1}. On the other hand, the mobile phase for the determination of uric acid concentration consists of 2% acetonitrile and 98% formic acid (0.1%) at a flow rate of 1 mL min^{−1}. In both cases, chromatographic separation is carried out with a Zorbax Eclipse Plus C-18 column (4.6 mm \times 100 mm, supplied from Agilent, Madrid, Spain), and the injection volume is 20 μ L.

Creatinine is determined by ion chromatography (IC) with a Metrohm 930 Compact IC Flex (Madrid, Spain) coupled to a conductivity detector. Urea and hydrogen peroxide concentrations are estimated by a spectrophotometric colorimetric method according to references [41,42], respectively, using a UV-1700 Shimadzu Spectrophotometer (Diusbur, Germany). Carboxylic acids formed during the degradation of PenG are identified by HPLC using a Jasco 2080 Plus equipped with a Hi-Plex (7.7 mm \times 300 mm, 8 μ m). The UV detection is set at 210 nm. The mobile phase consists of 5 mM H₂SO₄ that flows at 0.8 mL min^{−1}, and the injection volume is 20.0 μ L. Mineralization is monitored through total organic carbon (TOC) using a Multi N/C 3100 Analytic Jena analyzer (Jena, Germany).

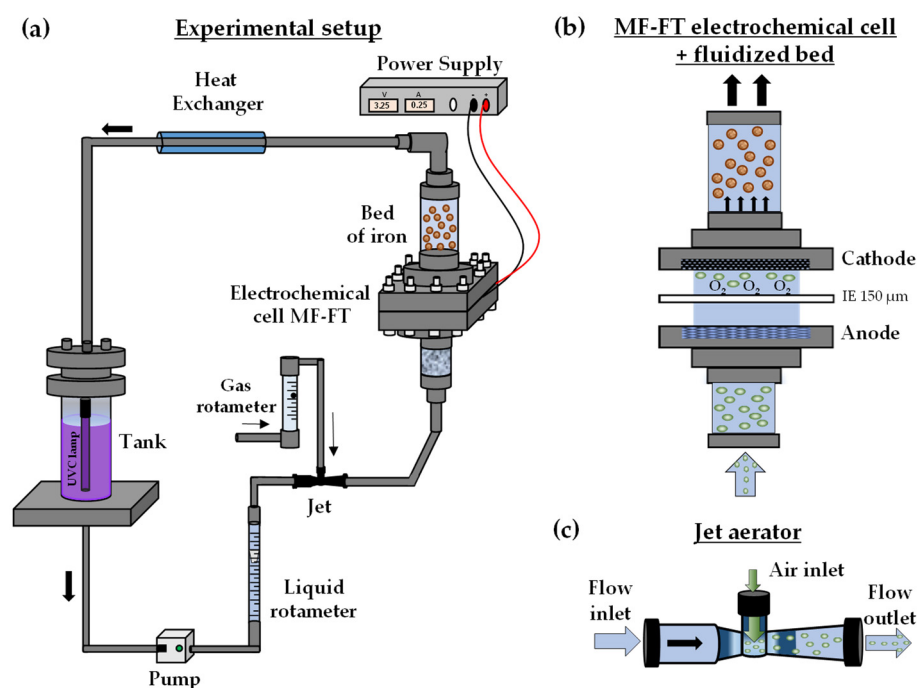


Figure 9. Experimental setup used in this work: (a) Complete view of the diagram; (b) Diagram of the MF-FT electrochemical cell and fluidized bed; (c) Diagram of the jet aerator.

In addition, the intermediate compounds of PenG degradation are identified with an Agilent 1260 series HPLC Infinity coupled to an Agilent time-of-flight mass spectrometer (LC–MS TOF 6320). It is operated in the electrospray positive ionization (ESI+) mode with the following conditions: capillary voltage to 3.5 kV, skimmer voltage to 65 V, gas temperature to 325 °C, nebulizer to 50 psi and drying gas to 10 L min^{−1}. Chromatographic separation is conducted by a Zorbax Eclipse Plus C-18 at a flow rate of 0.6 mL min^{−1} at 25 °C. The mobile phase consists of 50% formic acid (0.1%) and 50% methanol. The injection volume is 10 μL.

3.4. Microbiological Analysis

3.4.1. Toxicity

The Microtox[®] M5000 Toxicity Analyzer (Modern Water, York, UK) is used to obtain the acute toxicity of the samples before and after treatment by the inhibition of bioluminescence of marine bacteria *Vibrio fischeri*, according to the instructions provided by the supplier. The osmotic control of the samples is adjusted prior to the tests. A decrease in luminescence implies a reduction in cellular respiration. The emitted bioluminescence is recorded for 15 min of exposure at 15 °C and is compared to that of the blank sample. The luminosity reduction data are processed to obtain a standardized value of inhibition.

3.4.2. Antibiotic Activity

The antibiotic activity of polluted urine samples is determined by using a Microtrac[®] 4200 (SY-LAB, Neupurkersdorf, Austria) that counts the colony forming units (CFU) per mL. The microorganism used as an indicator is *E. faecalis* (ATCC 19433) supplied by CECT, Valencia, Spain. Before the antibiotic activity assay, bacteria are incubated at 37 °C for 10–24 h using the culture medium Tryptone Soy Agar ISO (Scharlab, Barcelona, Spain). Subsequently, the urine is contaminated with 10⁶–10⁷ CFU mL^{−1} *E. faecalis*. After this, the assays are conducted in a beaker under continuous agitation (150 rpm) and temperature (37 °C), where the samples are added to the solution containing the microorganism for 3 h. Additionally, a control sample is collected to determine the initial concentration of the microorganisms. Once the test time has elapsed, the samples are introduced into the

equipment to perform the CFU count. Each sample is measured in quadruplicate (without dilution and up to 1:1000 dilution).

3.5. Short-Term Biochemical Oxygen Demand

For short-term biochemical oxygen demand (BOD_{ST}), unacclimated activated sludge is used (from a local conventional wastewater treatment plant). The sludge maintains aeration for more than one night in the absence of external substrate addition in the bioreactor at 20 ± 3 °C. The tests are conducted in a glass beaker (150 mL) with 95 mL of activated sludge and 5 mL of sample under continuous agitation. Before the BOD_{ST} test, the pH values are adjusted to 7.0, and 2 drops of a nitrification inhibitor (N-allylthiourea, 98% from Sigma-Aldrich, Madrid, Spain) are added to avoid the nitrification of compounds present in urine, such as urea and ammonium. With regard to dissolved oxygen decay ($mg\ O_2\ dm^{-3}$), the BOD_{ST} is estimated as the difference between the dissolved oxygen concentration of the endogenous phase before and after adding the sample to the sludge. The dissolved oxygen concentration (DO) is monitored by using an oximeter (OX 4100H, pHenomenal® from VWR, Llinars del Vallès, Spain).

4. Conclusions

This work demonstrates that PenG can be efficiently and selectively removed by EF, reaching low mineralization. The type of anode material (BDD or MMO) plays a very important role in the efficiency of the process for PenG degradation. The percentages of PenG removal in the EF process are 100% and 75.5% when BDD and MMO are used as anodes, respectively. In addition, the presence of other organic compounds in urine decreases the efficiency of the process due to competitive oxidation. After EF treatment, the biodegradability increases from 0.16 to approximately $0.8\ mg\ O_2\ dm^{-3}$, and the toxicity decreases to 30–15% depending on the electrodes used. However, the antibiotic effect (estimated in terms of *E. faecalis* inhibition) remains above 90% with MMO-EF and 45% with BDD-EF. This may be related to the nature of the intermediates accumulated in the reaction system in each case. Finally, the coupling of UVC light to the system significantly improves the EF process. Thus, PEF-MMO/Foam shows a synergy coefficient of 166% (two times higher than that of PEF-BDD/Foam) and an improvement in the removal of the antibiotic effect of approximately 89.00%. This means that PEF can be efficiently used as a pretreatment for WWTPs to decrease the chemical risk of complex solutions polluted with antibiotics.

Supplementary Materials: The following supporting information can be downloaded at: <https://www.mdpi.com/article/10.3390/catal12060602/s1>, Figure S1. Evolution of Pen G concentration (C/C_0) with the electric charge passed during the EF of Pen G solutions ($50\ mg\ dm^{-3}$) in 50 mM sodium sulfate medium (●) or urine (■). Onset: Evolution of the concentration of the main organics present in urine medium: urea (○), creatinine (◇) and uric acid (Δ). Experimental conditions: $j = 5\ mA\ cm^{-2}$, $pH_0 = 3.0$, MMO as anode and titanium foam with CB/PTFE as cathode; Table S1. Composition of the synthetic urine.

Author Contributions: Conceptualization: Á.M., E.L., M.A.R. and C.S.; methodology: Á.M.; validation: E.L., M.A.R. and C.S.; formal analysis: Á.M. and C.S.; investigation: Á.M.; resources: P.C., M.A.R. and C.S.; data curation: Á.M.; writing—original draft preparation: Á.M.; writing—review and editing: E.L. and C.S.; supervision: M.A.R. and C.S.; project administration: P.C. and C.S.; funding acquisition: P.C. and C.S. All authors have read and agreed to the published version of the manuscript.

Funding: This research was funded by the Ministry of Science and Innovation (MCIN/AEI/10.13039/501100011033/) through grants PID2019-110904RB-I00 and EQC2018-004469-P.

Data Availability Statement: Not applicable.

Conflicts of Interest: The authors declare no conflict of interest.

References

1. Patel, M.; Kumar, R.; Kishor, K.; Mlsna, T.; Pittman, C.U.; Mohan, D. Pharmaceuticals of Emerging Concern in Aquatic Systems: Chemistry, Occurrence, Effects, and Removal Methods. *Chem. Rev.* **2019**, *119*, 3510–3673. [[CrossRef](#)] [[PubMed](#)]
2. Bampos, G.; Petala, A.; Frontistis, Z. Recent Trends in Pharmaceuticals Removal from Water Using Electrochemical Oxidation Processes. *Environments* **2021**, *8*, 85. [[CrossRef](#)]
3. Gonzaga, I.M.D.; Moratalla, A.; Eguiluz, K.I.B.; Salazar-Banda, G.R.; Cañizares, P.; Rodrigo, M.A.; Saez, C. Novel Ti/RuO₂/IrO₂ anode to reduce the dangerousness of antibiotic polluted urines by Fenton-based processes. *Chemosphere* **2021**, *270*, 129344. [[CrossRef](#)] [[PubMed](#)]
4. Arslan-Alaton, I.; Caglayan, A.E. Toxicity and biodegradability assessment of raw and ozonated procaine penicillin G formulation effluent. *Ecotoxicol. Environ. Saf.* **2006**, *63*, 131–140. [[CrossRef](#)]
5. El-Ghenemy, A.; Rodríguez, R.M.; Brillas, E.; Oturan, N.; Oturan, M.A. Electro-Fenton degradation of the antibiotic sulfanilamide with Pt/carbon-felt and BDD/carbon-felt cells. Kinetics, reaction intermediates, and toxicity assessment. *Environ. Sci. Pollut. Res.* **2014**, *21*, 8368–8378. [[CrossRef](#)]
6. Goulart, L.A.; Moratalla, A.; Lanza, M.R.V.; Saez, C.; Rodrigo, M.A. Photocatalytic performance of Ti/MMO/ZnO at degradation of levofloxacin: Effect of pH and chloride anions. *J. Electroanal. Chem.* **2021**, *880*, 114894. [[CrossRef](#)]
7. Paulus, G.K.; Hornstra, L.M.; Alygizakis, N.; Slobodnik, J.; Thomaidis, N.; Medema, G. The impact of on-site hospital wastewater treatment on the downstream communal wastewater system in terms of antibiotics and antibiotic resistance genes. *Int. J. Hyg. Environ. Health* **2019**, *222*, 635–644. [[CrossRef](#)]
8. Hama Aziz, K.H.; Omer, K.M.; Mahyar, A.; Miessner, H.; Mueller, S.; Moeller, D. Application of Photocatalytic Falling Film Reactor to Elucidate the Degradation Pathways of Pharmaceutical Diclofenac and Ibuprofen in Aqueous Solutions. *Coatings* **2019**, *9*, 465. [[CrossRef](#)]
9. Hama Aziz, K.H.; Miessner, H.; Mueller, S.; Kalass, D.; Moeller, D.; Khorshid, I.; Rashid, M.A.M. Degradation of pharmaceutical diclofenac and ibuprofen in aqueous solution, a direct comparison of ozonation, photocatalysis, and non-thermal plasma. *Chem. Eng. J.* **2017**, *313*, 1033–1041. [[CrossRef](#)]
10. Cordeiro, S.G.; Ziem, R.; Schweizer, Y.A.; Costa, B.; Kuhn, D.; Haas, P.; Weber, A.C.; Heidrich, D.; Ethur, E.M.; Steffens, C.; et al. Degradation of micropollutant cephalixin by ultraviolet (UV) and assessment of residual antimicrobial activity of transformation products. *Water Sci. Technol.* **2021**, *84*, 374–383. [[CrossRef](#)]
11. Mirzaei, A.; Chen, Z.; Haghghat, F.; Yerushalmi, L. Removal of pharmaceuticals from water by homo/heterogeneous Fenton-type processes—A review. *Chemosphere* **2017**, *174*, 665–688. [[CrossRef](#)] [[PubMed](#)]
12. Moratalla, Á.; Cotillas, S.; Lacasa, E.; Cañizares, P.; Rodrigo, M.A.; Sáez, C. Electrochemical Technologies to Decrease the Chemical Risk of Hospital Wastewater and Urine. *Molecules* **2021**, *26*, 6813. [[CrossRef](#)] [[PubMed](#)]
13. Gonzaga, I.M.D.; Moratalla, A.; Eguiluz, K.I.B.; Salazar-Banda, G.R.; Cañizares, P.; Rodrigo, M.A.; Saez, C. Influence of the doping level of boron-doped diamond anodes on the removal of penicillin G from urine matrixes. *Sci. Total Environ.* **2020**, *736*, 139536. [[CrossRef](#)]
14. Sordello, F.; Fabbri, D.; Rapa, L.; Minero, C.; Minella, M.; Vione, D. Electrochemical abatement of cefazolin: Towards a viable treatment for antibiotic-containing urine. *J. Clean. Prod.* **2021**, *289*, 125722. [[CrossRef](#)]
15. Feng, L.; Serna-Galvis, E.A.; Oturan, N.; Giannakis, S.; Torres-Palma, R.A.; Oturan, M.A. Evaluation of process influencing factors, degradation products, toxicity evolution and matrix-related effects during electro-Fenton removal of piroxicam from waters. *J. Environ. Chem. Eng.* **2019**, *7*, 103400. [[CrossRef](#)]
16. Bello, M.M.; Abdul Raman, A.A.; Asghar, A. A review on approaches for addressing the limitations of Fenton oxidation for recalcitrant wastewater treatment. *Process Saf. Environ. Prot.* **2019**, *126*, 119–140. [[CrossRef](#)]
17. Liu, N.; Xie, H.; Wei, J.; Li, Y.; Wang, J.; Yu, N.; Zhao, N.; Zhang, L.; Chen, Z. Catalytic activity of a composite metal electrode catalyst for the degradation of real dyeing wastewater by a heterogeneous electro-Fenton process. *J. Environ. Chem. Eng.* **2019**, *7*, 102930. [[CrossRef](#)]
18. Davarnejad, R.; Azizi, J. Alcoholic wastewater treatment using electro-Fenton technique modified by Fe₂O₃ nanoparticles. *J. Environ. Chem. Eng.* **2016**, *4*, 2342–2349. [[CrossRef](#)]
19. Farshchi, M.E.; Aghdasinia, H.; Khataee, A. Modeling of heterogeneous Fenton process for dye degradation in a fluidized-bed reactor: Kinetics and mass transfer. *J. Clean. Prod.* **2018**, *182*, 644–653. [[CrossRef](#)]
20. Anotai, J.; Su, C.-C.; Tsai, Y.-C.; Lu, M.-C. Effect of hydrogen peroxide on aniline oxidation by electro-Fenton and fluidized-bed Fenton processes. *J. Hazard. Mater.* **2010**, *183*, 888–893. [[CrossRef](#)]
21. Pérez, J.F.; Llanos, J.; Sáez, C.; López, C.; Cañizares, P.; Rodrigo, M.A. The jet aerator as oxygen supplier for the electrochemical generation of H₂O₂. *Electrochim. Acta* **2017**, *246*, 466–474. [[CrossRef](#)]
22. Yu, F.; Zhou, M.; Yu, X. Cost-effective electro-Fenton using modified graphite felt that dramatically enhanced on H₂O₂ electro-generation without external aeration. *Electrochim. Acta* **2015**, *163*, 182–189. [[CrossRef](#)]
23. Pérez, J.F.; Sáez, C.; Llanos, J.; Cañizares, P.; López, C.; Rodrigo, M.A. Improving the Efficiency of Carbon Cloth for the Electrogeneration of H₂O₂: Role of Polytetrafluoroethylene and Carbon Black Loading. *Ind. Eng. Chem. Res.* **2017**, *56*, 12588–12595. [[CrossRef](#)]
24. Pérez, J.F.; Llanos, J.; Sáez, C.; López, C.; Cañizares, P.; Rodrigo, M.A. Towards the scale up of a pressurized-jet microfluidic flow-through reactor for cost-effective electro-generation of H₂O₂. *J. Clean. Prod.* **2019**, *211*, 1259–1267. [[CrossRef](#)]

25. Yu, F.; Chen, Y.; Pan, Y.; Yang, Y.; Ma, H. A cost-effective production of hydrogen peroxide via improved mass transfer of oxygen for electro-Fenton process using the vertical flow reactor. *Sep. Purif. Technol.* **2020**, *241*, 116695. [[CrossRef](#)]
26. Ridruejo, C.; Centellas, F.; Cabot, P.L.; Sirés, I.; Brillas, E. Electrochemical Fenton-based treatment of tetracaine in synthetic and urban wastewater using active and non-active anodes. *Water Res.* **2018**, *128*, 71–81. [[CrossRef](#)] [[PubMed](#)]
27. Panizza, M.; Cerisola, G. Direct and mediated anodic oxidation of organic pollutants. *Chem. Rev.* **2009**, *109*, 6541–6569. [[CrossRef](#)]
28. Yu, X.; Zhou, M.; Hu, Y.; Groenen Serrano, K.; Yu, F. Recent updates on electrochemical degradation of bio-refractory organic pollutants using BDD anode: A mini review. *Environ. Sci. Pollut. Res. Int.* **2014**, *21*, 8417–8431. [[CrossRef](#)]
29. Espinoza, C.; Romero, J.; Villegas, L.; Cornejo-Ponce, L.; Salazar, R. Mineralization of the textile dye acid yellow 42 by solar photoelectro-Fenton in a lab-pilot plant. *J. Hazard. Mater.* **2016**, *319*, 24–33. [[CrossRef](#)]
30. Garcia-Segura, S.; Anotai, J.; Singhadech, S.; Lu, M.-C. Enhancement of biodegradability of o-toluidine effluents by electro-assisted photo-Fenton treatment. *Process Saf. Environ. Prot.* **2017**, *106*, 60–67. [[CrossRef](#)]
31. Santos, G.d.O.S.; Eguiluz, K.I.B.; Salazar-Banda, G.R.; Saez, C.; Rodrigo, M.A. Testing the role of electrode materials on the electro-Fenton and photoelectro-Fenton degradation of clopyralid. *J. Electroanal. Chem.* **2020**, *871*, 114291. [[CrossRef](#)]
32. Goulart, L.A.; Moratalla, A.; Cañizares, P.; Lanza, M.R.V.; Sáez, C.; Rodrigo, M.A. High levofloxacin removal in the treatment of synthetic human urine using Ti/MMO/ZnO photo-electrocatalyst. *J. Environ. Chem. Eng.* **2022**, *10*, 107317. [[CrossRef](#)]
33. Santos, G.O.S.; Gonzaga, I.M.D.; Eguiluz, K.I.B.; Salazar-Banda, G.R.; Saez, C.; Rodrigo, M.A. Improving biodegradability of clopyralid wastes by photoelectrolysis: The role of the anode material. *J. Electroanal. Chem.* **2020**, *864*, 114084. [[CrossRef](#)]
34. Moratalla, Á.; Araújo, D.M.; Moura, G.O.M.A.; Lacasa, E.; Cañizares, P.; Rodrigo, M.A.; Sáez, C. Pressurized electro-Fenton for the reduction of the environmental impact of antibiotics. *Sep. Purif. Technol.* **2021**, *276*, 119398. [[CrossRef](#)]
35. Cotillas, S.; Lacasa, E.; Herraiz, M.; Sáez, C.; Cañizares, P.; Rodrigo, M.A. The Role of the Anode Material in Selective Penicillin G Oxidation in Urine. *ChemElectroChem* **2019**, *6*, 1376–1384. [[CrossRef](#)]
36. Herraiz-Carboné, M.; Cotillas, S.; Lacasa, E.; Moratalla, Á.; Cañizares, P.; Rodrigo, M.A.; Sáez, C. Improving the biodegradability of hospital urines polluted with chloramphenicol by the application of electrochemical oxidation. *Sci. Total Environ.* **2020**, *725*, 138430. [[CrossRef](#)] [[PubMed](#)]
37. Sun, K.; Xu, W.; Lin, X.; Tian, S.; Lin, W.F.; Zhou, D.; Sun, X. Electrochemical Oxygen Reduction to Hydrogen Peroxide via a Two-Electron Transfer Pathway on Carbon-Based Single-Atom Catalysts. *Adv. Mater. Interfaces* **2021**, *8*, 2001360. [[CrossRef](#)]
38. Pérez, J.F.; Llanos, J.; Sáez, C.; López, C.; Cañizares, P.; Rodrigo, M.A. On the design of a jet-aerated microfluidic flow-through reactor for wastewater treatment by electro-Fenton. *Sep. Purif. Technol.* **2019**, *208*, 123–129. [[CrossRef](#)]
39. Martínez-Huitle, C.A.; Panizza, M. Electrochemical oxidation of organic pollutants for wastewater treatment. *Curr. Opin. Electrochem.* **2018**, *11*, 62–71. [[CrossRef](#)]
40. Cotillas, S.; de Vidales, M.J.M.; Llanos, J.; Sáez, C.; Cañizares, P.; Rodrigo, M.A. Electrolytic and electro-irradiated processes with diamond anodes for the oxidation of persistent pollutants and disinfection of urban treated wastewater. *J. Hazard. Mater.* **2016**, *319*, 93–101. [[CrossRef](#)]
41. Gonzaga, I.M.D.; Dória, A.R.; Moratalla, A.; Eguiluz, K.I.B.; Salazar-Banda, G.R.; Cañizares, P.; Rodrigo, M.A.; Saez, C. Electrochemical systems equipped with 2D and 3D microwave-made anodes for the highly efficient degradation of antibiotics in urine. *Electrochim. Acta* **2021**, *392*, 139012. [[CrossRef](#)]
42. Monteiro, M.K.S.; Moratalla, Á.; Sáez, C.; Dos Santos, E.V.; Rodrigo, M.A. Production of Chlorine Dioxide Using Hydrogen Peroxide and Chlorates. *Catalysts* **2021**, *11*, 1478. [[CrossRef](#)]